# A teleoperation framework for mobile robots based on shared control

Article (Accepted Version)

# A Teleoperation Framework for Mobile Robots based on Shared Control

Jing Luo†, Zhidong Lin†, Yanan Li, and Chenguang Yang⋆

***Abstract*—Mobile robots can complete a task in cooperation with a human partner. In this paper, a hybrid shared control method for a mobile robot with omnidirectional wheels is proposed. A human partner utilizes a six degrees of freedom haptic device and electromyography (EMG) signals sensor to control the mobile robot. A hybrid shared control approach based on EMG and artificial potential field is exploited to avoid obstacles according to the repulsive force and attractive force and to enhance the human perception of the remote environment based on force feedback of the mobile platform. This shared control method enables the human partner to tele-control the mobile robot's motion and achieve obstacles avoidance synchronously. Compared with conventional shared control methods, this proposed one provides a force feedback based on muscle activation and drives the human partners to update their control intention with predictability. Experimental results demonstrate the enhanced performance of the mobile robots in comparison with the methods in the literature.**

***Index Terms*—Hybrid shared control, force feedback, human control intention, human-robot interaction, mobile robots.**

## I. Introduction

APPLICATIONS of mobile robots have penetrated every aspect of human society [1] [2], such as in industry, agriculture, and military surveillance, etc. Due to the limitation of current technology and resource, mobile robots cannot work in full autonomy in many uncertain environments [3]. So far, human intervention is still largely required in applications of mobile robots. In many scenarios, a human partner can control the mobile robots through a teleoperation interface to perform a collaborative task [4] [5].

Manuscript received: September, 9, 2019; Revised November, 22, 2019; Accepted December, 6, 2019.

This paper was recommended for publication by Editor Allison M. Okamura upon evaluation of the Associate Editor and Reviewers' comments. This work was partially supported by the Engineering and Physical Sciences Research Council (EPSRC) under Grant EP/S001913, and UK-China Joint Research and Innovation Partnership Fund PhD Placement Programme 201806150139.

J. Luo is with the Key Laboratory of Autonomous Systems and Networked Control, College of Automation Science and Engineering, South China University of Technology, Guangzhou, 510640, China, and also with the Department of Bioengineering, Imperial College of Science Technology and Medicine, London SW7 2AZ, U.K.

Z. Lin is with the Key Laboratory of Autonomous Systems and Networked Control, College of Automation Science and Engineering, South China University of Technology, Guangzhou, 510640, China.

Y. Li is with the Department of Engineering and Design, University of Sussex, Brighton BN1 9RH, UK.

C. Yang is with Bristol Robotics Laboratory, University of the West of England, Bristol BS16 1QY, UK. † Contributed Equally.

⋆Corresponding author is C. Yang. Email: cyang@ieee.org.

Digital Object Identifier (DOI): see top of this page.

For a teleoperated mobile robots, its control strategies can be updated according to user intention, leading to shared control methods. Shared control schemes are often combined with other control methods in practice. For example, in [6], shared control with adaptive servo method is presented to assist disabled people to complete a transport task which integrates a tracking controller and an obstacle avoidance controller. In a complex environment, outputs of a compliance motion control and autonomous navigation control are combined to form the inputs of a shared controller [7]. Furthermore, force feedback of the mobile robots is usually used to help human partner to improve the perception of environments for enhancing the operation skills [8], [9]. Obstacle avoidance is one of the most important tasks in the research area of the mobile robots. When a mobile robot follows the commands of a human partner to a target position, it must avoid the obstacles autonomously at the same time. In the literature, dynamical systems approach [10], decentralized cooperative mean method [11], and viable velocity obstacle with motion planning algorithm [12], and artificial potential field (APF) method [13], are successfully developed to deal with this issue. Indeed, these algorithms can achieve a superior performance, but they are designed from the human's point of view. In other words, mobile robots "passively" cooperate with the human partner. For improving the performance of human-robot interaction, it is essential to make the mobile robots "actively" cooperate with the human partner according to human's control intention.

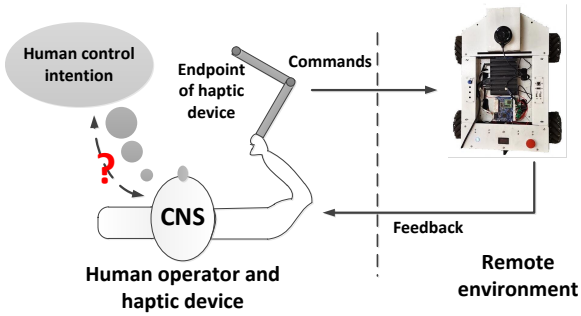


Fig. 1. How to catch the human control intention and deliver it to the robots? .

As is shown in Fig. 1, how to catch the human control intention and deliver it to the mobile robots? It is demonstrated that humans can adjust their muscle co-contraction to

update the machanical impedance of arm in the interaction with unstable or stable environments [14] [15]. This updating mechanism is regulated by human central neural system (CNS). The CNS enables humans to modulate their impedance flexibly with superior capabilities through changing the muscle activation. In fact, electromyography (EMG) signals can reflect the muscle activation which is regulated by the CNS [16] [17]. Thus, EMG profile can be regarded as a representation to indicate the human control intention [18]. The EMG-based methods can be integrated with Kinect sensor [19] [20] and inertial measure unit sensor to achieve human control of mobile robots or omnidirectional wheelchairs [21] [22]. However, these approaches are developed based on machine learning, so it is hard to use them for control of mobile robots in real time. Moreover, EMG-based muscle activation is not directly used in control applications. In our previous works, stiffness control based on EMG signals is proposed to provide a natural human-robot cooperative control interface [23] [24], and to present a quantitative solution for human intention estimation [25].

However, those previous human-robot cooperative control strategies can not provide effective force feedback and ensure obstacle avoidance by accounting human control intention. In this paper, we utilize the strategy of CNS based human control to develop a teleoperation framework for mobile robots. Based on the APF method in [9], a hybrid shared control with EMG-based component is developed to avoid the obstacles and to improve the bidirectional human-robot perception using force feedback. This force feedback provides the human partner good awareness to skillfully control the mobile robots when it gets close to the obstacles. Validation of the enhanced teleoperated control framework is performed in the experimental environments using a haptic device with 6 degrees of freedom (DoFs), and a mobile platform.

The rest of this paper is organized as follows. At first, preliminary information about dynamics of a mobile platform and processing of EMG signals is presented in Section II. Section III describes the proposed framework. Then, the experimental results are explained in Section IV. Finally, conclusion is given in Section V.

## II. Preliminaries

In the preliminaries section, dynamics of a mobile platform, processing of EMG signals, and message communication between robot operation system (ROS) Master, haptic device, and EMG signal capture device are described.

### A. Dynamics of mobile platform

Fig. 2 shows the configuration of the mobile platform. It can be seen that the mobile platform contains a body and four omnidirectional wheels. For the omnidirectional wheel [26], its velocity along X-axis $v_{xs,i}$ can be defined as

$$v_{xs,i} = v_{w_i} + v_i \frac{1}{\sqrt{2}} \tag{1}$$

where $v_{w_i}$ represents the velocity of the $i$th omnidirectional wheel. $v_i$ denotes the velocity of roller $i$, $i = 1, 2, 3, 4$. Considering the difference in relative positions for four wheels, the velocities along X-axis are represented in different forms. One has

$$\begin{cases} v_{xs,1} = v_{t,x} - wL_a \\ v_{xs,2} = v_{t,x} + wL_a \\ v_{xs,3} = v_{t,x} - wL_a \\ v_{xs,4} = v_{t,x} + wL_a \end{cases} \tag{2}$$

with

$$L_a = r_{mp} cos\theta_{mp} \tag{3}$$

where $v_{t,x}$ denotes the speed of X-axis for the mobile platform. $w$ is the angular velocity about the yaw axis.

Correspondingly, the velocities along Y-axis of mobile platform are

$$\begin{cases} v_{ys,1} = v_i \frac{1}{\sqrt{2}} = v_{t,y} + wL_b, i = 1 \\ v_{ys,2} = -v_i \frac{1}{\sqrt{2}} = v_{t,y} + wL_b, i = 2 \\ v_{ys,3} = -v_i \frac{1}{\sqrt{2}} = v_{t,y} - wL_b, i = 3 \\ v_{ys,4} = v_i \frac{1}{\sqrt{2}} = v_{t,y} - wL_b, i = 4 \end{cases} \tag{4}$$

with

$$L_b = R_{mp} sin\theta_{mp} \tag{5}$$

where $v_{t,y}$ denotes the speed of Y-axis for the mobile platform.

Then, we can obtain the velocities $\{v_{w_i}, i = 1, 2, 3, 4\}$ of mobile platform

$$\begin{bmatrix} v_{w_1} \\ v_{w_2} \\ v_{w_3} \\ v_{w_4} \end{bmatrix} = K_{mp} \begin{bmatrix} w \\ v_{t,x} \\ v_{t,y} \end{bmatrix} \tag{6}$$

with

$$K_{mp} = \begin{bmatrix} -L_a - L_b & 1 & -1 \\ L_a + L_b & 1 & 1 \\ -L_a - L_b & 1 & 1 \\ L_a + L_b & 1 & -1 \end{bmatrix} \tag{7}$$

where $K_{mp}$ is a 4×3 matrix.

According to the relationship between velocity and angular velocity, the angular velocity of the mobile platform $\{w_{w_i}, i = 1, 2, 3, 4\}$ can be represented as

$$\begin{bmatrix} w_{w_1} \\ w_{w_2} \\ w_{w_3} \\ w_{w_4} \end{bmatrix} = r_{mp}^{-1} K_{mp} R^{-1} \begin{bmatrix} \dot{\theta} \\ \dot{x} \\ \dot{y} \end{bmatrix} \tag{8}$$

with

$$R = \begin{bmatrix} 1 & 0 & 0 \\ 0 & cos\theta & -sin\theta \\ 0 & sin\theta & cos\theta \end{bmatrix} \tag{9}$$

where $r_{mp}$ is the radius of omnidirectional wheel. $R$ represents the rotation matrix between the mobile platform coordinate system and the world coordinate system. $x$ and $y$ are the representations of world frame. $\theta$ denotes orientation of the mobile platform.

The parameters of the mobile platform can be seen in Table I.

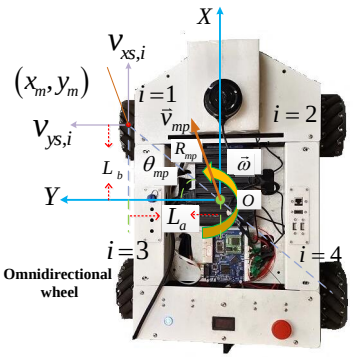


Fig. 2. Configuration of the mobile platform.

TABLE I
PARAMETERS OF THE MOBILE PLATFORM.

| | |
|---|---|
| $x_m$, $y_m$ | Positions of mobile platform. |
| $v_{xs,i}$, $v_{sy,i}$ | Velocities of omnidirectional wheel. |
| $\theta_{mp}$ | Angle inclined from the geometric center. |
| $R_{mp}$ | Distance between the center of mass and center of omnidirectional wheel. |
| $\overrightarrow{v}_{mp}$ | Velocity of mobile platform. |
| $\overrightarrow{w}$ | Angular velocity of yaw axis rotation. |

### B. Processing of EMG signals

In this paper, we utilize an EMG sensor to capture the muscle activation. The EMG signal $u_{emg}$ can be presented as

$$u_{emg} = \sum_{i}^{N} u(i), \quad i = 1, 2, 3, ...N \tag{10}$$

where $u(i)$ denotes the captured raw EMG signals. $N$ represents the number of channels of the EMG sensor.

In order to obtain the muscle activation accurately, the EMG signals should be filtered through moving average, low pass filter and envelope.

After filtering of EMG signals, the muscle activation based on EMG signals can be presented as below

$$a(i) = \sqrt{\frac{1}{w_{win}} \sum_{i=1}^{w_{win}} u_i^2} \quad i = 1, 2, ...w_{win} \tag{11}$$

where $a(i)$ denotes the muscle activation. $w_{win}$ represents the moving window's length. The value of $w_{win}$ can be determined based on experience.

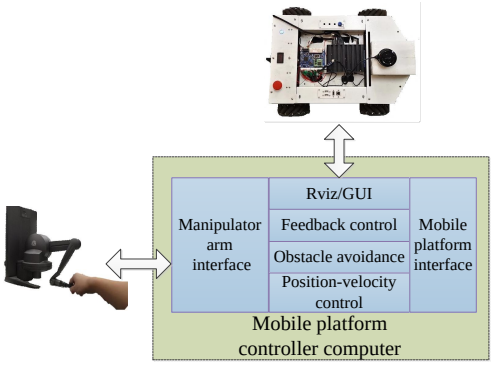


Fig. 3. Control architecture of the mobile robot.

## III. PROPOSED FRAMEWORK

The control structure of the mobile robot is shown in Fig. 3. The mobile platform is controlled at task level with position-velocity control and feedback control. The communication mode is described in the following.

### A. System constitution

Fig. 5 shows the framework constitution of the system. On the master side, the human partner wears an EMG sensor and moves a haptic device to teleoperate the remote mobile robot. The EMG sensor is used to capture EMG signals to reflect muscle activation. The haptic device sends positions and velocities to the remote mobile platform by a movable stylus in the Cartesian workspace.

The remote robot contains a mobile platform with four omnidirectional wheels and is controlled in a teleoperation mode. A hybrid shared control scheme with force feedback is proposed for the mobile platform to achieve obstacle avoidance and to enable the human partner to adapt their control intention. In the following, we will present the corresponding methods in detail.

### B. Message communication

The teleoperation system utilizes STM32 microcontroller to control the mobile platform. The mobile platform connects with the controller and EMG signal capture device through WIFI technique. The message communication of the proposed teleoperation system and mobile robot's model in simulator Rviz are shown in Fig. 4. In the ROS system, multiple functions can be achieved via ROS MASTER, such as $Base\_controller$, $Robot\_description$, $User\_interface$ etc.

### C. Motion control

The rotation angle of mobile platform $\alpha_{mp}$ is presented as

$$\alpha_{mp} = tan(\frac{y_m}{x_m}) \tag{12}$$

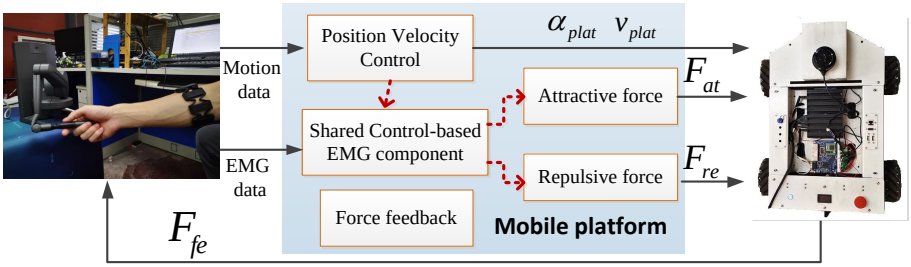


Fig. 5. Framework constitution of the mobile service robots.

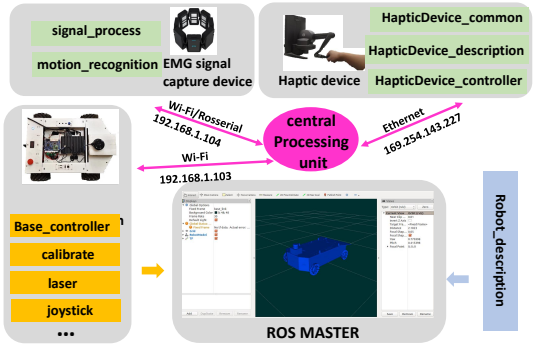


Fig. 4. Message communication and the mobile robot's model in simulator Rviz. In the overall teleoperated system, mobile platform communicates with the central processing unit with IP addresses. EMG signal capture device works on Windows and communicates with the ROS through rosserial.

where $y_m$ and $x_m$ denote the positions in Y-axis and X-axis for haptic device, respectively.

Velocity of mobile platform can be presented as

$$v_{mp} = K_{plat}(z_m - z_{min}) + v_{min} \tag{13}$$

with

$$K_{plat} = \frac{v_{max} - v_{min}}{z_{max} - z_{min}} \tag{14}$$

where $K_{plat}$ is a factor to map the velocity of the mobile platform. $z_{max}$ and $z_{min}$ represent the maximum and minimum of position of the haptic device in Z-axis. $v_{max}$ and $v_{min}$ are the maximum and minimum of speed of the mobile platform, which can be obtained by a pilot experiment beforehand.

As noted above, we can find that Z-axis of the haptic device is used to control the velocity of the mobile platform, X-axis and Y-axis are used to describe the motion profile of the mobile platform, therefore, there is a transformation matrix to describe the relationship between the frame of haptic device and the frame of the mobile platform. The transformation matrix can be represented as below.

$$R^{'} = \begin{bmatrix} 1 & 0 & 0 \\ 0 & 1 & 0 \\ 0 & 0 & 0 \end{bmatrix} \tag{15}$$

### D. Hybrid shared control

When the mobile platform moves to the target place through a teleoperation mode, it is inevitable that the platform encounters an obstacle. When the mobile platform gets close to the obstacle, the human partner controls it to avoid the obstacle as soon as possible. In this stage, the muscle activation can directly reflect the human control intention.

Specifically, in the presence of an obstacle, the mobile platform receives a resultant force (a repulsive force and an attractive force) based on the hybrid shared control method to drive the mobile platform away from the obstacle. In this process, the haptic device can receive a force feedback (Eq. (23)) and provide a stimuli to the human partner. At the same time, the force feedback can make the mobile platform move away from the obstacle.

Inspired by [24], we develop a linear function to describe the EMG-based component, which can be defined as

$$K_{emg} = K^0(a_i - a_{max}) + K^0_{min} \tag{16}$$

with

$$K^0 = \frac{K^0_{max} - K^0_{min}}{a_{min} - a_{max}} \tag{17}$$

where $K^0$ represents the scale parameter of human factor to adjust the muscle activation and $K^0_{max} \geq K_{emg} \geq K^0_{min}$ is a proportionality coefficient to represent the influence of EMG-based component. $a_{max} \geq a_i \geq a_{min}$ denotes the muscle activation [27].

For Eqs. (16) and (17), it is noted that when the human partner receives the force feedback through the haptic device, he/she will change his/her manipulation to avoid the obstacle, and the muscle activation (EMG) will change. The EMG can change the values of the repulsive force and the attractive force in the hybrid shared control. In specific, when the mobile platform moves towards the obstacle, the muscle activation transfers to a proportionality coefficient to increase the resultant force to achieve a quick avoidance of the obstacle.

It is noted that the EMG signal is just utilized in the proposed approach, so it is not necessary to do the muscle specialized training. The operation with EMG sensor is the same as the ordinary teleoperation.

Naturally, we use a hybrid shared control scheme which combines APF and EMG-based component for the mobile platform in Fig. 6. In this scheme, the mobile platform's motion is determined by a resultance force in the force field. This resultance force contains a repulsive force and an attractive force. The repulsive force propels the platform away from the obstacle. And the attractive force makes the platform move to the target position. The APF of hybrid shared control $Q_{to}$ can be represented as [28], [29]

$$Q_{to} = Q_{at} + Q_{re} \tag{18}$$

with

$$Q_{at} = \frac{1}{2}(\mu_1 + K_{emg}) f^2(p, p_{go}) \tag{19}$$

where $Q_{at}$ denotes the hybrid gravitational potential field function. $Q_{re}$ is the hybrid repulsive potential field function. $\mu_1$ is the gravitational gain parameter. $f(p, p_{go})$ represents the distance from the goal to the mobile platform, where $p_{go}$ is the goal's position.

$$Q_{re} = \begin{cases} \frac{1}{2}(\mu_2 + K_{emg}) \\ \quad (\frac{1}{f(p, p_{ob})} - \frac{1}{f_0})^2, & f(p, p_{ob}) \le f_0 \\ \quad 0, & f(p, p_{ob}) > f_0 \end{cases} \tag{20}$$

where $\mu_2$ is the repulsion gain parameter. $f_0$ is the influence radius for each obstacle.

Correspondingly, the attractive force can be defined as

$$\begin{aligned} F_{at} &= -\nabla\ Q_{at} \\ &= (\mu_1 + K_{emg}) f(p, p_{go}) \frac{\partial f}{\partial p} \end{aligned} \tag{21}$$

The repulsive force can be defined as

$$\begin{aligned} F_{re} &= -\nabla\ Q_{re} \\ &= \begin{cases} (\mu_2 + K_{emg})(\frac{1}{f(p, p_{ob})} - \frac{1}{f_0}) \\ \qquad \frac{1}{f^2(p, p_{ob})} \frac{\partial f}{\partial p}, & f(p, p_{ob}) \le f_0 \\ \qquad 0, & f(p, p_{ob}) > f_0 \end{cases} \end{aligned} \tag{22}$$

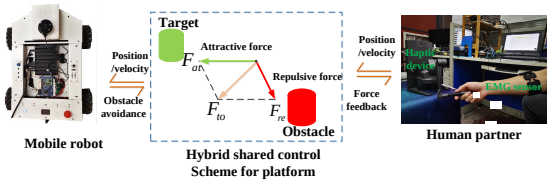


Fig. 6. Hybrid shared control scheme for mobile platform.

### E. Force feedback

There is a distance between the mobile platform and the obstacle in the process of the mobile platform moving to the target position. As shown in Fig. 7, when this distance

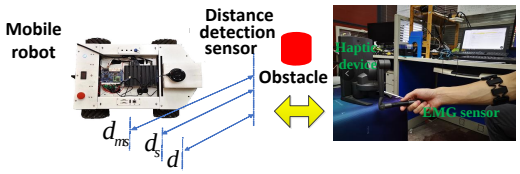


Fig. 7. Force feedback generation for the mobile platform.

$d$ is less than a safe distance $d_s$, the mobile platform can generate a force feedback to the human operator through the haptic device (as in Eq. (23)). The human operator can change his/her commands to control the mobile platform.

$$F_{fe} = \begin{cases} (K_{fe} + K_{emg})(d_{mw} - d), & d \le d_s \\ 0, & d > d_s \end{cases} \tag{23}$$

where $K_{fe}$ is a positive gain parameter for the platform. $d_{mw}$ and $d_s$ are the maximum of warning distance and safe distance, respectively. It can be concluded that when the distance is smaller, the force feedback of mobile platform is greater.

In the paper, the low-level control of the haptic device and the mobile platform is a proportional-derivative (PD) controller. The EMG-based component is transferred to a coefficient $K_{emg} > 0$, which adapts the control parameters of PD controller. If the parameters of PD controller are positive definite, the stability of the closed-loop system can be guaranteed [24]. It is noted that the haptic device with a human partner and the mobile platform is a typical teleoperation system. As its passivity is not affected by the proposed approach, the stability can be guaranteed [30].

## IV. Experiments and Results

In this section, we experimentally demonstrate the performance and robustness of the proposed enhanced teleoperated control method in different environments.

### A. Experiment setup

The experimental platform is built to evaluate the effectiveness of the proposed framework.

A MYO armband (Thalmic Labs Inc. made) is utilized to capture the EMG signals in the process of teleoperation. Touch X is used as a haptic device to control the mobile platform and the manipulator arm through WIFI technique. All devices are performed on the ROS and Windows environment. The haptic device Touch X has six DoFs but only three axes in linear motion have force feedback. For the haptic device, the greater the force is in a direction, the harder it is to move in that direction. It is noted that the human partner wears the EMG sensor on the same arm. A laser radar is mounted on the body of the mobile platform.

The experimental environments are shown in Fig. 8. Fig. 8(a) shows the experimental environment for one obstacle. Fig. 8(b) shows that there are four independent

cardboard boxes as the experimental environment in the multi-obstacle experiment. The human partner tele-controls the mobile platform to move and avoid the obstacles in an indoor environment. It is noted that the target position is $(350cm, -40cm)$, and operation errors of the human partner of X-axis and Y-axis are limited to $\pm 5cm$ and $\pm 10cm$.

(a) One-obstacle environment. (b) Multi-obstacles environment.

Fig. 8. Experimental environment.

### B. Obstacle avoidance experiment

These obstacle experiments are performed in two different conditions: hybrid shared control with EMG-based component and without EMG-based component. The parameters of shared control are set as $\mu_1 = 100$, $\mu_2 = 100$, $K_{fe} = 1$. In the experimental results, $-c1$ and $-c2$ indicate the results without EMG-based component and with EMG-based component, respectively.

*1) Case 1: one-obstacle environment:* Fig. 9 shows the performance of obstacle avoidance using hybrid shared control in one-obstacle environment ((Fig. 8(a)).

The resultant force and feedback force can be seen in Figs. 9(a)-9(b). Fx-c1, Fy-c1 and Fx-c2, Fy-c2 are the resultant forces in X-axis and Y-axis in the case with EMG-based component and without EMG-based component. Fig. 9(a) indicates that when the mobile platform is controlled without EMG-based component, the mobile platform suffers from a small resultant force in the process of obstacle avoidance. In comparison, the mobile platform achieves a better performance of obstacle avoidance under the condition with EMG-based component. It is noted that the resultant forces in X-axis for these two conditions are set as 150N. The resultant force is larger than that of mobile platform without EMG-based component. Especially, when the mobile platform passes by the obstacle, the haptic device can receive a larger feedback force with EMG-based component in comparison with that without EMG-based component in Fig. 9(b). The resultant force and feedback force can drive the mobile platform to move away from the obstacle.

Fig. 9(c) shows rotation angle in the process of obstacle avoidance. Since the number of crest and trough of the rotation angle is related to the number of the obstacles, so it can be seen that the first trough of the curves indicates the obstacle in the one-obstacle environment. We have marked the starting point of obstacle avoidance, which shows that the method with EMG-based component can achieve obstacle avoidance in advance in comparison with that without EMG-based component.

Fig. 9(d) shows the velocity performance in the process of obstacle avoidance. It can be seen that the velocity is more continuous in the case with EMG-based component (blue curve) in comparison with that without EMG-based component (red curve). Fig. 9(e) indicates the actual path in one-obstacle environment.

The muscle activation of human partner can be seen in Fig. 9(f). The muscle activation changes abruptly at about 24s when the mobile platform gets close to the obstacle. In this sense, we can see that the muscle activation varies with the process of obstacle avoidance and EMG-based component can enhance the performance of obstacle avoidance.

Table II shows the total time and displacement of total path travelled in the task of obstacle avoidance. It can be found that the completion times with EMG-based component and without EMG-based component are 58.4510s and 64.9429s, respectively. Similarly, the total displacement in the case with EMG-based component is shorter than that without EMG-based component. The maximum of warning distance indicates the minimum of safe distance between the mobile platform and the obstacle. It is noted that the maximum of warning distance is an absolute value regardless of the coordinate point. Since the maximum of warning distance changes in the process of obstacle avoidance, we utilize its average value to indicate the minimum safe distance.

In addition, from Table II, we can see that the minimum of safe distance in the case with EMG-based component is greater than that without EMG-based component. It can be concluded that the proposed method based on EMG-based component can achieve a greater minimum of safe distance.

TABLE II
TOTAL TIME, DISPLACEMENT OF TOTAL PATH TRAVELLED, AND AVERAGE MINIMUM OF SAFE DISTANCE IN THE ONE OBSTACLE EXPERIMENT.

| Parameters | Without-EMG | With-EMG |
|---|---|---|
| **Total time [Sec]** | 64.9429 | 58.4510 |
| **Total displacement [cm]** | 179.4354 | 157.9623 |
| **Minimum safe distance [cm]** | 79.23 | 80.55 |

*2) Case 2: multi-obstacle experiment:* In order to test the robustness and performance of the proposed approach, we experimentally demonstrate the method in the multi-obstacle environment (Fig. 8(b)). The experimental parameters are set the same as in Case 1. Fig. 10 and Table III show the performance of the proposed method in the multi-obstacle environment. It can be seen that the EMG-based method can achieve a better performance of obstacle avoidance in comparison with that without EMG-based component, in terms of minimal safe distance, resultant force, and force feedback. Furthermore, the hybrid shared control method can predict the obstacle through the resultant force and feedback force and provides a relatively longer process to compel the mobile platform to move away from the obstacles.

Similarly, from Table III, it can be seen that the total time and total displacement are shorter in the case with EMG-

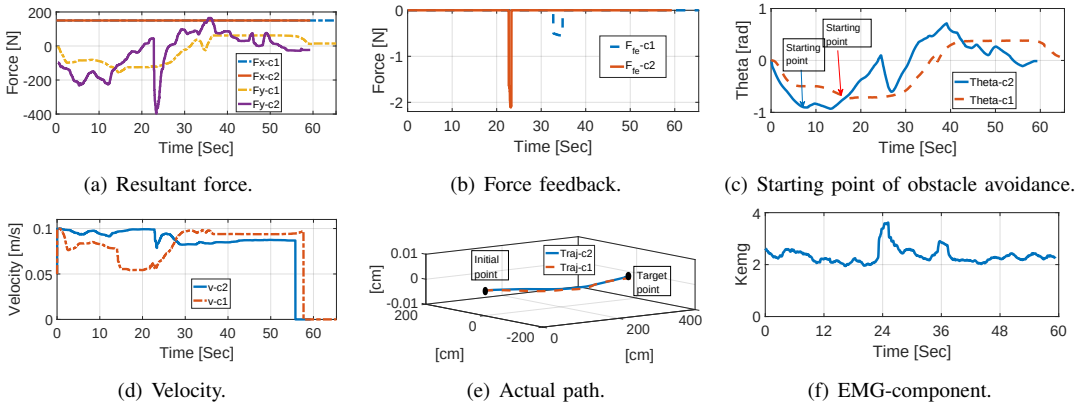


(a) Resultant force. (b) Force feedback. (c) Starting point of obstacle avoidance.

(d) Velocity. (e) Actual path. (f) EMG-component.

Fig. 9. Performance comparison with/without EMG-component in the one obstacle experiment.

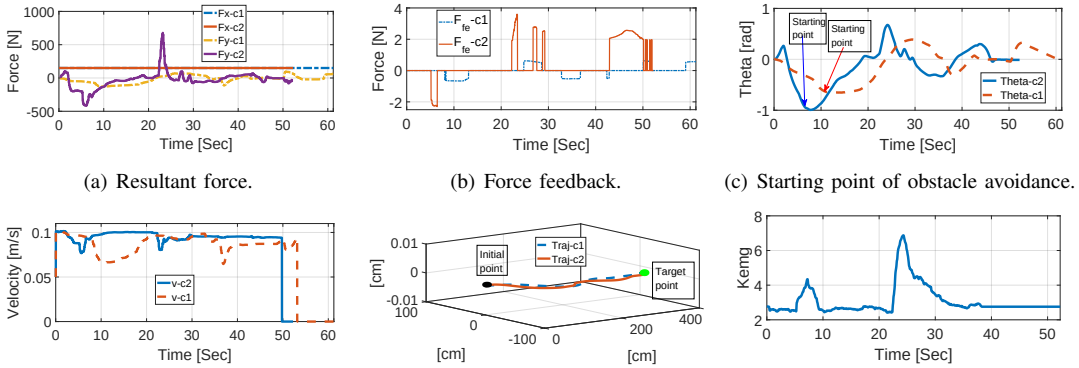


(a) Resultant force. (b) Force feedback. (c) Starting point of obstacle avoidance.

(d) Velocity. (e) Actual path. (f) EMG-component.

Fig. 10. Performance comparison with/without EMG-component in the multi-obstacle experiment.

based component in comparison with that without EMG-based component.

TABLE III
TOTAL TIME, DISPLACEMENT OF TOTAL PATH TRAVELLED, AND AVERAGE MINIMUM OF SAFE DISTANCE IN THE MULTI-OBSTACLE EXPERIMENT.

| Parameters | Without-EMG | With-EMG |
|---|---|---|
| **Total time [Sec]** | 60.8470 | 51.7560 |
| **Total displacement [cm]** | 182.3736 | 154.8775 |
| **Minimum safe distance [cm]** | 55.08 | 57.53 |

## V. CONCLUSION

In this paper, we develop a hybrid shared control approach to avoid obstacles for the teleoperated system. The hybrid shared control scheme integrated with both APF and EMG-based component could provide a relatively larger resultant force to make the mobile platform stay away from the obstacles in comparison with traditional APF method. Furthermore, the EMG-based component incorporates the impacts of human factor through the CNS human motor control mechanism. The experimental results demonstrate the effectiveness of the proposed enhanced teleoperation framework.

Compared to the traditional obstacle avoidance methods [13] [28] [31], the resultant force and force feedback are more responsive, as the mobile robots can effectively account the influence of human control intention. To emphasize, when adding the EMG-based component, the mobile robot can update the attractive force and repulsive force according to the muscle activation and generate a corresponding force feedback to the human partner to achieve "active" collaboration with the human partner. Based on the experimental results, the proposed hybrid shared control scheme can achieve predictability for avoiding obstacles and provides a force feedback to the human partner to update their control commands. Specifically, EMG signal is a reflection of peripheral neural system controlled by CNS. In this paper, we utilize the EMG signal to reflect the status of the human partner. The EMG component is transferred to a proportionality coefficient to increase the resultant force of the hybrid shared control when the mobile platform moves toward an obstacle. In addition, the haptic device can receive a force feedback to inform the human partner the existence of the obstacles. The force feedback can make the mobile platform move toward the obstacle more difficult. At the same time, the human partner can control the robot with the force feedback from the haptic device. In this sense, the human operator's

workload can be reduced. The applications of the proposed work can be used to search and rescue, remote inspection, etc. In a case of multiple obstacles, the mobile platform will calculate the minimum distance between the mobile platform and obstacles. Then the mobile platform can achieve obstacle avoidance according to the minimum distance and the resultant force. The use of the human partner's EMG signals is the same as in the case of one obstacle.

It is noted that a certain level of teleoperation skill is needed, no matter the CNS is involved or not. However, it is necessary to use the mechanism of CNS to learn the human control intention or skill and to decrease the reliance of operation skill [32] [33]. In this sense, this topic is the focus of this work. The robustness of the proposed method is one research topic in the future study. Since the control distance is not too far, there is no issue of time delay noticed in our experiments. However, when the distance reaches a certain range, the issue of time delay can not be ignored. Therefore, the long distance control problem with time delay is another future work.

## REFERENCES


[1] R. Siegwart, I. R. Nourbakhsh, and D. Scaramuzza, *Introduction to autonomous mobile robots*. MIT press, 2011.

[2] M. Cross, K. A. McIsaac, B. Dudley, and W. Choi, "Negotiating corners with teleoperated mobile robots with time delay," *IEEE Transactions on Human-Machine Systems*, vol. 48, no. 6, pp. 682–690, 2018.

[3] C. W. Nielsen, M. A. Goodrich, and R. W. Ricks, "Ecological interfaces for improving mobile robot teleoperation," *IEEE Transactions on Robotics*, vol. 23, no. 5, pp. 927–941, 2007.

[4] N. J. Cooke, "Human factors of remotely operated vehicles," in *Proceedings of the Human Factors and Ergonomics Society Annual Meeting*, vol. 50, pp. 166–169, SAGE Publications Sage CA: Los Angeles, CA, 2006.

[5] N. Enayati, G. Ferrigno, and E. De Momi, "Skill-based human–robot cooperation in tele-operated path tracking," *Autonomous Robots*, vol. 42, no. 5, pp. 997–1009, 2018.

[6] H. Wang and X. P. Liu, "Adaptive shared control for a novel mobile assistive robot," *IEEE/ASME Transactions on Mechatronics*, vol. 19, no. 6, pp. 1725–1736, 2014.

[7] S.-Y. Jiang, C.-Y. Lin, K.-T. Huang, and K.-T. Song, "Shared control design of a walking-assistant robot," *IEEE Transactions on Control Systems Technology*, vol. 25, no. 6, pp. 2143–2150, 2017.

[8] P. Nadrag, L. Temzi, H. Arioui, and P. Hoppenot, "Remote control of an assistive robot using force feedback," in *2011 15th International Conference on Advanced Robotics (ICAR)*, pp. 211–216, IEEE, 2011.

[9] Y. Xu, C. Yang, X. Liu, and Z. Li, "A teleoperated shared control scheme for mobile robot based semg," in *2018 3rd International Conference on Advanced Robotics and Mechatronics (ICARM)*, pp. 288–293, IEEE, 2018.

[10] T. Machado, T. Malheiro, S. Monteiro, W. Erlhagen, and E. Bicho, "Multi-constrained joint transportation tasks by teams of autonomous mobile robots using a dynamical systems approach," in *2016 IEEE international conference on robotics and automation (ICRA)*, pp. 3111–3117, IEEE, 2016.

[11] J. Jin, Y.-G. Kim, S.-G. Wee, and N. Gans, "Decentralized cooperative mean approach to collision avoidance for nonholonomic mobile robots," in *2015 IEEE International Conference on Robotics and Automation (ICRA)*, pp. 35–41, IEEE, 2015.

[12] Z. Liu, Z. Jiang, T. Xu, H. Cheng, Z. Xie, and L. Lin, "Avoidance of high-speed obstacles based on velocity obstacles," in *2018 IEEE International Conference on Robotics and Automation (ICRA)*, pp. 7624–7630, IEEE, 2018.

[13] C. W. Warren, "Global path planning using artificial potential fields," in *Proceedings, 1989 International Conference on Robotics and Automation*, pp. 316–321, IEEE, 1989.

[14] E. Burdet, R. Osu, D. W. Franklin, T. E. Milner, and M. Kawato, "The central nervous system stabilizes unstable dynamics by learning optimal impedance," *Nature*, vol. 414, no. 6862, p. 446, 2001.

[15] D. W. Franklin, R. Osu, E. Burdet, M. Kawato, and T. E. Milner, "Adaptation to stable and unstable dynamics achieved by combined impedance control and inverse dynamics model," *Journal of neurophysiology*, vol. 90, no. 5, pp. 3270–3282, 2003.

[16] T. F. BESIER, D. G. LLOYD, and T. R. ACKLAND, "Muscle activation strategies at the knee during running and cutting maneuvers," *Medicine & Science in Sports & Exercise*, vol. 35, no. 1, pp. 119–127, 2003.

[17] D. W. Franklin, E. Burdet, K. P. Tee, R. Osu, C.-M. Chew, T. E. Milner, and M. Kawato, "Cns learns stable, accurate, and efficient movements using a simple algorithm," *Journal of neuroscience*, vol. 28, no. 44, pp. 11165–11173, 2008.

[18] J. Han, Q. Ding, A. Xiong, and X. Zhao, "A state-space emg model for the estimation of continuous joint movements," *IEEE Transactions on Industrial Electronics*, vol. 62, no. 7, pp. 4267–4275, 2015.

[19] B. Wang, C. Yang, and Q. Xie, "Human-machine interfaces based on emg and kinect applied to teleoperation of a mobile humanoid robot," in *Proceedings of the 10th World Congress on Intelligent Control and Automation*, pp. 3903–3908, IEEE, 2012.

[20] B. Wang, Z. Li, W. Ye, and Q. Xie, "Development of human-machine interface for teleoperation of a mobile manipulator," *International Journal of Control, Automation and Systems*, vol. 10, no. 6, pp. 1225–1231, 2012.

[21] M. T. Wolf, C. Assad, M. T. Vernacchia, J. Fromm, and H. L. Jethani, "Gesture-based robot control with variable autonomy from the jpl biosleeve," in *2013 IEEE International Conference on Robotics and Automation*, pp. 1160–1165, IEEE, 2013.

[22] A. S. Kundu, O. Mazumder, P. K. Lenka, and S. Bhaumik, "Hand gesture recognition based omnidirectional wheelchair control using imu and emg sensors," *Journal of Intelligent & Robotic Systems*, vol. 91, no. 3-4, pp. 529–541, 2018.

[23] C. Yang, J. Luo, Y. Pan, Z. Liu, and C.-Y. Su, "Personalized variable gain control with tremor attenuation for robot teleoperation," *IEEE Transactions on Systems, Man, and Cybernetics: Systems*, vol. 48, no. 10, pp. 1759–1770, 2017.

[24] J. Luo, C. Yang, N. Wang, and M. Wang, "Enhanced teleoperation performance using hybrid control and virtual fixture," *International Journal of Systems Science*, vol. 50, no. 3, pp. 451–462, 2019.

[25] J. Luo, C. Liu, and C. Yang, "Estimation of emg-based force using a neural-network-based approach," *IEEE Access*, vol. 7, pp. 64856–64865, 2019.

[26] V. Alakshendra and S. S. Chiddarwar, "Design of robust adaptive controller for a four wheel omnidirectional mobile robot," in *2015 International Conference on Advances in Computing, Communications and Informatics (ICACCI)*, pp. 63–68, IEEE, 2015.

[27] D. G. Lloyd and T. F. Besier, "An emg-driven musculoskeletal model to estimate muscle forces and knee joint moments in vivo," *Journal of biomechanics*, vol. 36, no. 6, pp. 765–776, 2003.

[28] S. S. Ge and Y. J. Cui, "New potential functions for mobile robot path planning," *IEEE Transactions on robotics and automation*, vol. 16, no. 5, pp. 615–620, 2000.

[29] J. Borenstein and Y. Koren, "Real-time obstacle avoidance for fast mobile robots," *IEEE Transactions on systems, Man, and Cybernetics*, vol. 19, no. 5, pp. 1179–1187, 1989.

[30] C. Yang, J. Luo, C. Liu, M. Li, and S.-L. Dai, "Haptics electromyogrphy perception and learning enhanced intelligence for teleoperated robot," *IEEE Transactions on Automation Science and Engineering*, vol. 16, no. 4, pp. 1512–1521, 2019.

[31] M. Rubagotti, T. Taunyazov, B. Omarali, and A. Shintemirov, "Semi-autonomous robot teleoperation with obstacle avoidance via model predictive control," *IEEE Robotics and Automation Letters*, vol. 4, no. 3, pp. 2746–2753, 2019.

[32] C. Yang, G. Ganesh, S. Haddadin, S. Parusel, A. Albu-Schaeffer, and E. Burdet, "Human-like adaptation of force and impedance in stable and unstable interactions," *IEEE transactions on robotics*, vol. 27, no. 5, pp. 918–930, 2011.

[33] G. Ganesh and E. Burdet, "Motor planning explains human behaviour in tasks with multiple solutions," *Robotics and Autonomous Systems*, vol. 61, no. 4, pp. 362–368, 2013.